Hepatic EPHX1 Potentiates Liver Fibrosis by Decreasing Eicosatrienoic Acids

Hiroko Ikenaga, Tsutomu Matsubara, Masaru Enomoto, Misako Sato-Matsubara, Le Thi Thanh Thuy, Ninh Quoc Dat, Truong Huu Hoang, Ngo Vinh Hanh, Kirara Inoue, Chiho Kadono, Hideki Fujii, Sawako Uchida-Kobayashi, Shogo Tanaka, Shoji Kubo, Takeaki Ishizawa, Daisuke Oikawa, Fuminori Tokunaga, Akihiro Tamori, Sergi Guixé-Muntet, Jordi Gracia-Sancho, Frank J Gonzalez, Kazuo Ikeda, and Norifumi Kawada

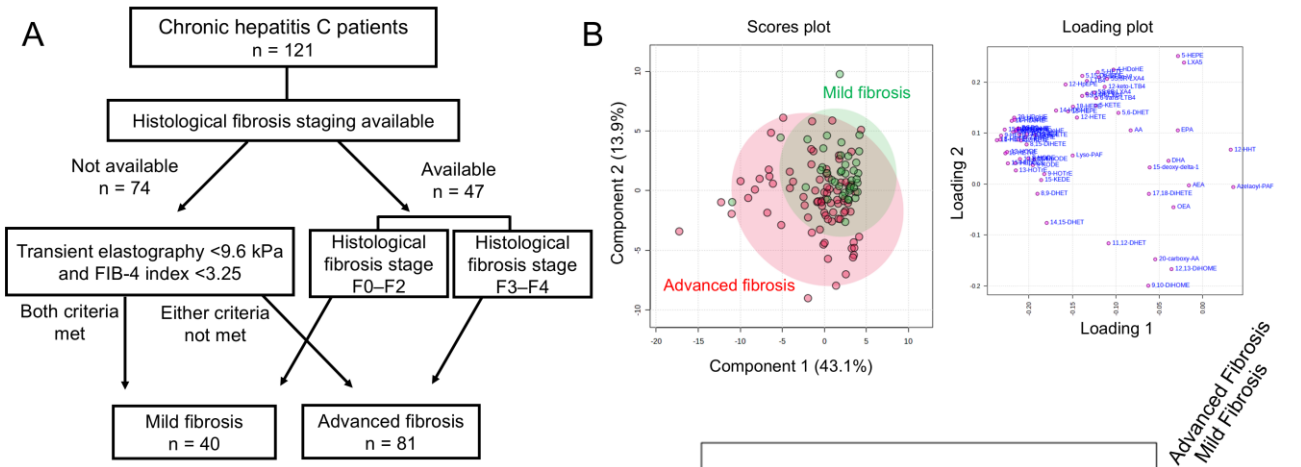
Table of Contents

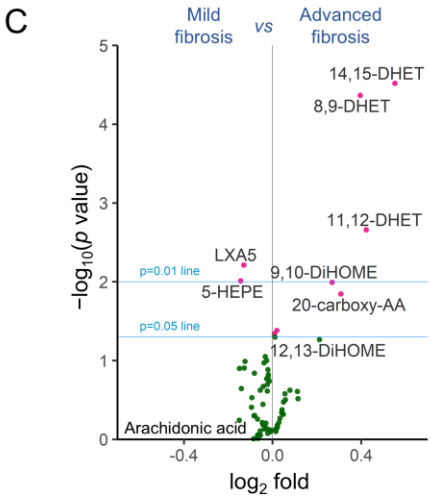
	Title	Page
Fig. S1	Lipidome analysis of samples from patients with chronic hepatitis C.	3 and 4
Fig. S2	Hepatic cytochrome P450 (CYP) 2C and 2J mRNA levels in patients with metabolic dysfunction-associated steatotic liver disease (MASLD).	5
Fig. S3	Hepatic microsomal epoxide hydrolase (EPHX1) and soluble epoxide hydrolase (EPHX2) protein levels in patients with chronic hepatitis C.	6 and 7
Fig. S4	Kinetic analysis of epoxyeicosatrienoic acid (EET) turnover in human microsomal and cytosolic fractions.	8 and 9
Fig. S5	Serum dihydroxyeicosatrienoic acid (DHET) levels in mouse models.	10
Fig. S6	Body weight, liver weight, serum ALT levels, hepatic gene expression, and immunohistochemical appearance against microsomal epoxide hydrolase (EPHX1) in high-fat, high-cholesterol (HFHC) diet-induced fibrotic mouse model.	11
Fig. S7	Hepatic microsomal epoxide hydrolase (EPHX1), soluble epoxide hydrolase (EPHX2), dihydroxyeicosatrienoic acid (DHET), and epoxyeicosatrienoic acid (EET) in methionine and choline-deficient (MCD) fibrotic mouse model.	12 and 13
Fig. S8	Hepatic epoxyeicosatrienoic acid (EET) and dihydroxyeicosatrienoic acid (DHET) levels, serum ALT levels, and hepatic Acta2 and alpha-smooth muscle actin (αSMA) expression in high-fat, high-cholesterol (HFHC)-fed Ephx1-null mice.	14
Fig. S9	Hepatic epoxyeicosatrienoic acid (EET) metabolism and liver fibrogenesis in thioacetamide (TAA)-administered Ephx1-null mice.	15 and 16
Fig. S10	Fibrotic gene expression in Effect of 11,12-epoxyeicosatrienoic acid (EET) on human hepatic stellate cells (HSCs).	17
Fig. S11	Effects of 14,15-epoxyeicosatrienoic acid (EET), 14,15-dihydroxyeicosatrienoic acid (DHET), 8,9-EET, and 8,9-DHET on human hepatic stellate cells (HSCs).	18 and 19
Fig. S12	Effects of 11,12-epoxyeicosatrienoic acid (EET) on signaling pathways in human hepatic stellate cells with or without transforming growth factor-β (TGF-β) stimulation.	20 and 21
Fig. S13	Effects of 11,12-epoxyeicosatrienoic acid (EET) on hepatic fibrogenic gene expression in thioacetamide (TAA)-induced liver fibrosis.	22
Fig. S14	Effects of 11,12-epoxyeicosatrienoic acid (EET) treatment after establishment of thioacetamide (TAA)-induced liver fibrosis.	23 and 24

Fig. S15	Cellular distribution of microsomal epoxide hydrolase 1 (EPHX1) in human and mouse liver.	25
Fig. S16	Single-cell RNA-sequencing analysis of Ephx1 expression in nonparenchymal liver cells from control and metabolic dysfunction-associated steatohepatitis (MASH) model mice.	26 and 27
Fig. S17	Effect of EPHX1 knockdown on 11,12-epoxyeicosatrienoic acid (EET) metabolism and fibrogenic response in human hepatic stellate cells (HSCs).	28
Table S1	Baseline patient characteristics for lipidome analysis in patients with MASLD.	29
Table S2	Baseline patient characteristics for lipidome analysis in patients with chronic hepatitis C.	30
Table S3	Univariate and multivariate logistic regression analyses of factors used to differentiate between chronic hepatitis C patients with or without advanced fibrosis.	31
Table S4	Baseline patient characteristics for immunohistochemistry staining in patients with MASLD.	32
Table S5	Baseline patient characteristics for immunohistochemistry staining in patients with chronic hepatitis C.	33
Table S6	Univariate and multivariate logistic regression analyses of factors used to differentiate between chronic hepatitis C patients with or without advanced fibrosis.	34
Table S7	Composition of CTRL and HFHC diets.	35
Table S8	Composition of CTRL and MCD diets.	36
Table S9	Chemicals used in this study.	37
Table S10	Antibodies used in this study.	38
Table S11	Primers used in this study.	39

Supplementary Figures

Fig. S1





D

Multivariate logistic regression analyses showing 11,12-DHETs predicted advanced fibrosis in chronic hepatitis C.				
Variables		OR	95%CI	*p* value
11,12-DHET	per 1 ng/mL	1.39	1.02–1.89	0.03*
BMI	per 1 kg/m^2	1.15	0.99–1.35	0.07
FIB-4 index	per 1	1.80	1.22–2.67	0.003**
Albumin	per 1 g/dL	0.14	0.03–0.69	0.02*
Bilirubin	per 1 mg/dL	7.57	0.91–63.3	0.06
ALT	per 10 U/L	0.98	0.89–1.08	0.70

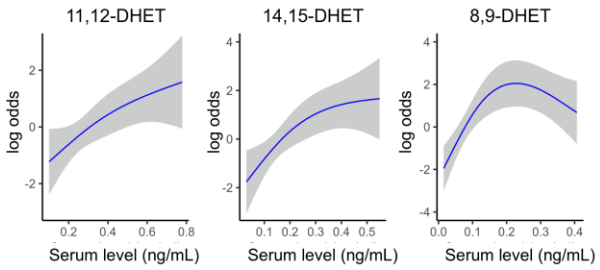


Fig. S1. Lipidome analysis of samples from patients with chronic hepatitis C. (A) Flowchart showing the design for lipidome analysis. (B) Partial least squares discriminant analysis score plots (left), loading plots (right), and metabolites with the highest VIP scores (lower). (C) Volcano plots for polyunsaturated fatty acid metabolites between groups. The x-axis represents the fold change (log2

21 scale), and the y-axis represents the *p* value (−log10 scale). (D) Results of multivariate logistic
22 regression models for predicting advanced fibrosis. The x-axis represents serum DHET levels, and the
23 y-axis represents the log odds calculated via logistic regression analysis for predicting advanced
24 fibrosis. Shaded area presents 95% confidence bounds. ALT, alanine aminotransferase; BMI, body
25 mass index; CI, confidence interval; DHET, dihydroxyeicosatrienoic acid; FIB-4, fibrosis-4: OR, odds
26 ratio; VIP, variable importance in projection. * $p < 0.05$, ** $p < 0.01$, *** $p < 0.001$.
27

Fig. S2

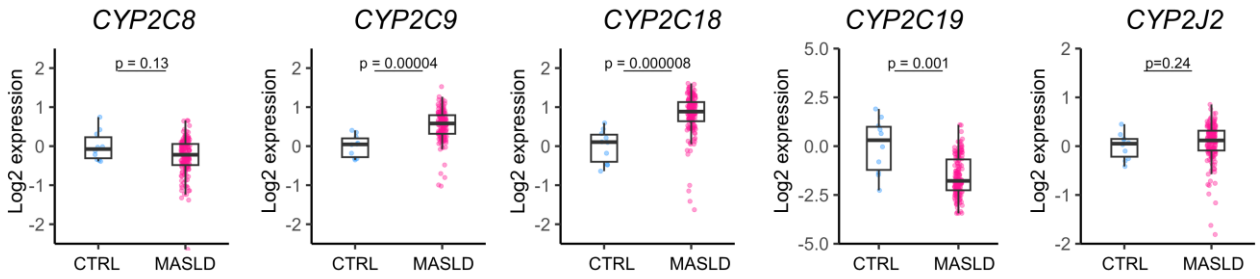
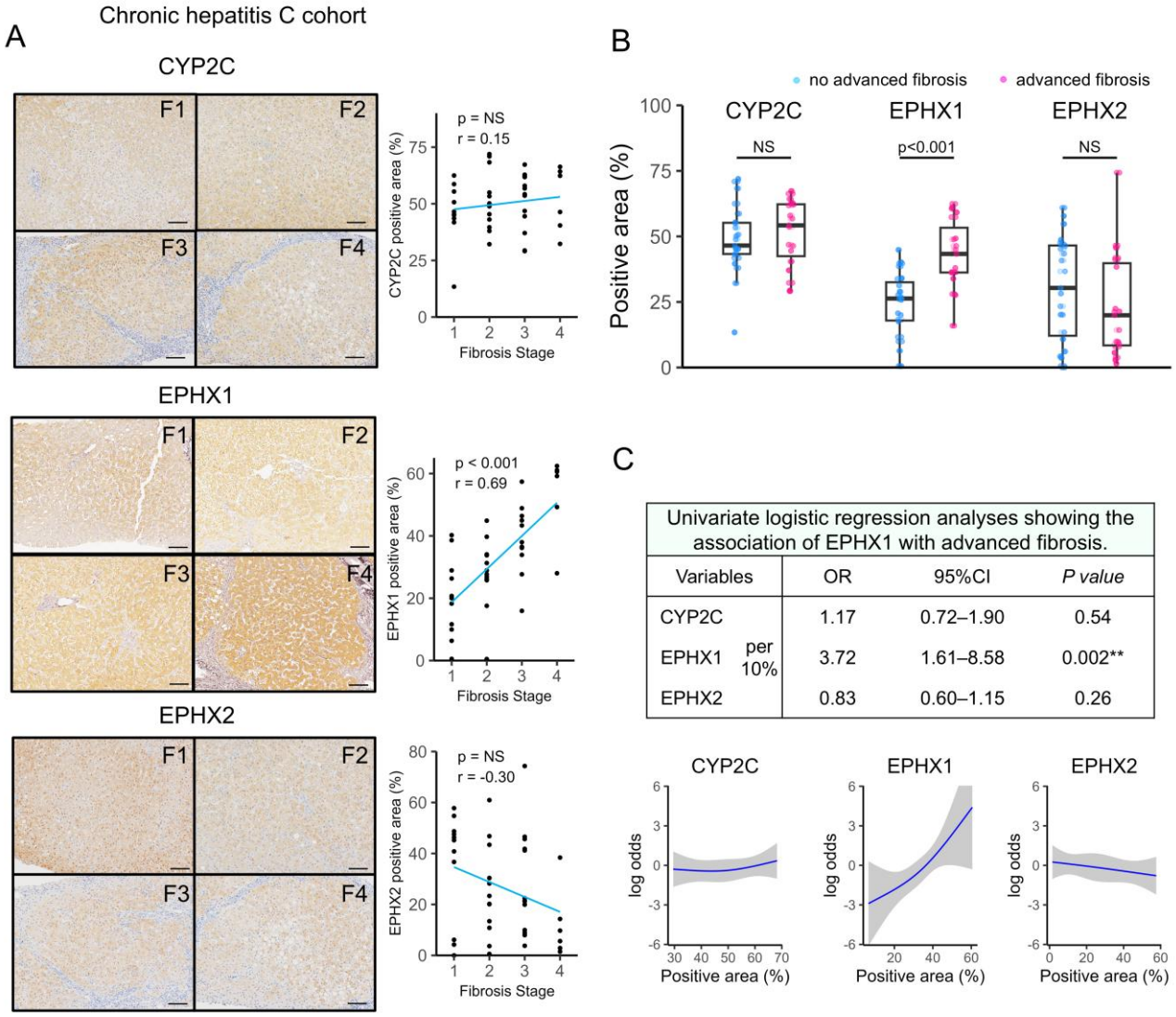


Fig. S2. Hepatic cytochrome P450 (CYP) 2C and 2J mRNA levels in patients with metabolic dysfunction-associated steatotic liver disease (MASLD). *CYP2C8*, *CYP2C9*, *CYP2C18*, *CYP2C19*, and *CYP2J2* mRNA levels in healthy controls and patients with MASLD. CTRL, control. Values were log2-transformed and centered to the control mean. Statistical significance was determined using the Mann–Whitney *U* test. NS, not significant. Boxes show the interquartile range (IQR), with median lines. Whiskers extend to the outermost values within 1.5×IQR of the box edges.

Fig. S3



Univariate logistic regression analyses showing the association of EPHX1 with advanced fibrosis.

Variables		OR	95%CI	*P value*
CYP2C		1.17	0.72–1.90	0.54
EPHX1	per 10%	3.72	1.61–8.58	0.002**
EPHX2		0.83	0.60–1.15	0.26

Fig. S3. Hepatic microsomal epoxide hydrolase (EPHX1) and soluble epoxide hydrolase (EPHX2) protein levels in patients with chronic hepatitis C.

(A) Immunohistochemical staining images of EPHX1 at each fibrosis stage and graphs of the correlation between liver fibrosis stage and cytochrome P450 (CYP) 2C, EPHX1 or EPHX2-positive area. Statistical significance was determined by Pearson's correlation test. Scale bar, 100 μm. (B) Quantification of immunohistochemical staining between patients with advanced fibrosis (fibrosis stage F3 or F4) and without advanced fibrosis. Statistical significance was determined using the Mann–Whitney *U* test. (C) Logistic regression analysis for predicting advanced fibrosis according to

the expression level of each enzyme. CI, confidence interval; OR, odds ratio. Boxes show the interquartile range (IQR), with median lines. Whiskers extend to the outermost values within 1.5×IQR of the box edges. * $p < 0.05$, ** $p < 0.01$, *** $p < 0.001$. NS, not significant.

Fig. S4

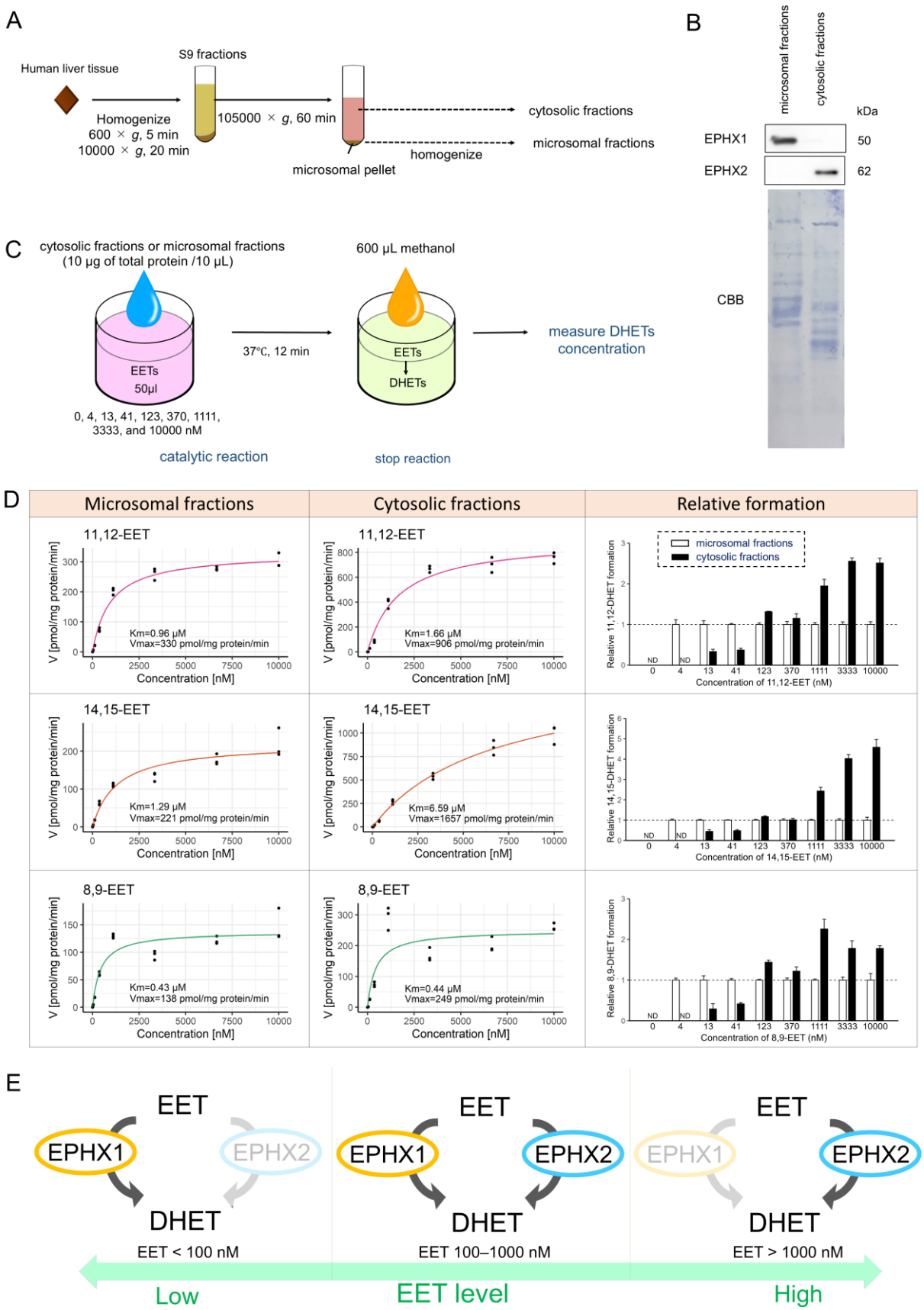

A
Human liver tissue
Homogenize
600 × g, 5 min
10000 × g, 20 min
S9 fractions
105000 × g, 60 min
microsomal pellet
homogenize
cytosolic fractions
microsomal fractions
B
microsomal fractions
cytosolic fractions
kDa
EPHX1
50
EPHX2
62
CBB
C
cytosolic fractions or microsomal fractions
(10 μg of total protein /10 μL)
EETs
50μl
0, 4, 13, 41, 123, 370, 1111,
3333, and 10000 nM
catalytic reaction
37℃, 12 min
600 μL methanol
EETs
DHETs
stop reaction
measure DHETs
concentration
D
Microsomal fractions
Cytosolic fractions
Relative formation
11,12-EET
Km=0.96 μM
Vmax=330 pmol/mg protein/min
Km=1.66 μM
Vmax=906 pmol/mg protein/min
microsomal fractions
cytosolic fractions
Relative 11,12-DHET formation
Concentration of 11,12-EET (nM)
14,15-EET
Km=1.29 μM
Vmax=221 pmol/mg protein/min
Km=6.59 μM
Vmax=1657 pmol/mg protein/min
Relative 14,15-DHET formation
Concentration of 14,15-EET (nM)
8,9-EET
Km=0.43 μM
Vmax=138 pmol/mg protein/min
Km=0.44 μM
Vmax=249 pmol/mg protein/min
Relative 8,9-DHET formation
Concentration of 8,9-EET (nM)
V [pmol/mg protein/min]
Concentration [nM]
ND
E
EET
EPHX1
EPHX2
DHET
EET < 100 nM
EET 100–1000 nM
EET > 1000 nM
Low
EET level
High

Fig. S4. Kinetic analysis of epoxyeicosatrienoic acid (EET) turnover in human microsomal and cytosolic fractions. (A) Scheme for the preparation of microsomal and cytosolic fractions from human liver. (B) Microsomal epoxide hydrolase (EPHX1) and soluble epoxide hydrolase (EPHX2) in microsomal and cytosolic fractions. Coomassie Brilliant Blue (CBB) staining was used to assess equal loading. (C) Scheme for kinetic analysis of EET metabolism. (D) Michaelis constant (*K*m) and maximum velocity of shortening (Vmax) were calculated using the Michaelis–Menten equation. The relative contributions of the microsomal and cytosolic fractions to EET hydrolysis are also presented. (E) Dominant enzyme for changes in EET between EPHX1 and EPHX2, depending on the concentration of EETs. UD, undetectable.

Fig. S5

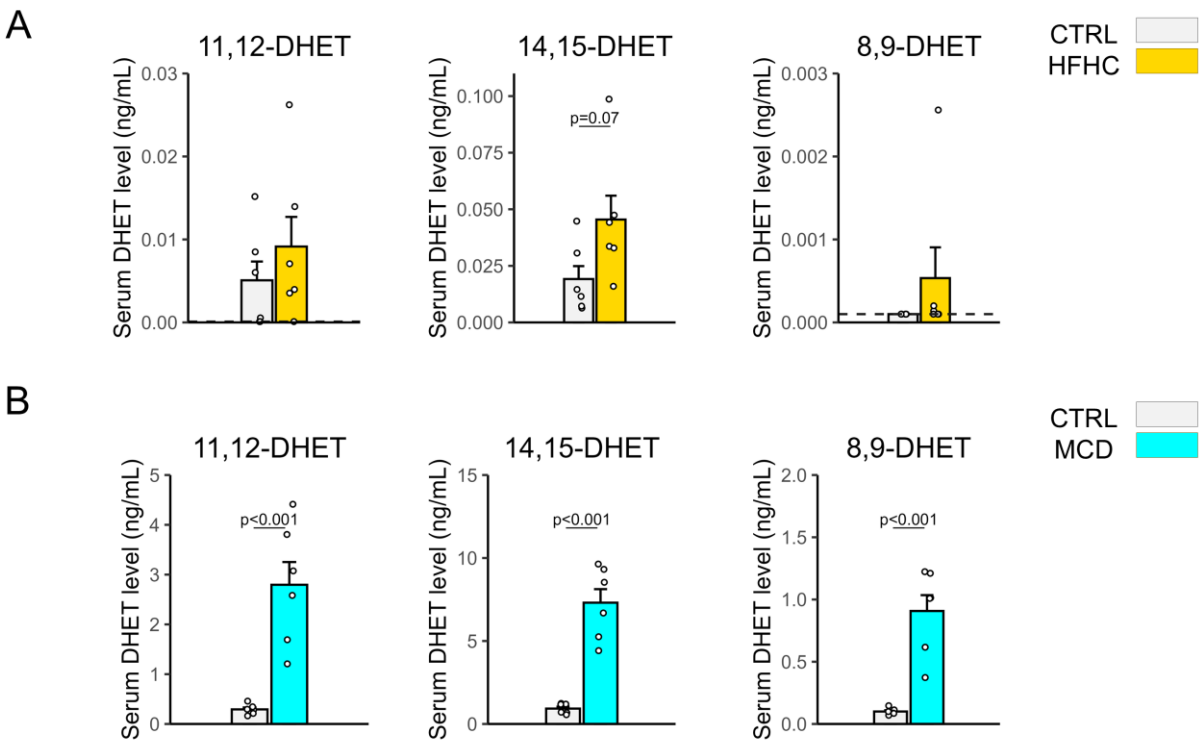


Fig. S5. Serum dihydroxyeicosatrienoic acid (DHET) levels in mouse models.

(A, B) Serum 11,12-DHET, 14,15-DHET, and 8,9-DHET levels in control (CTRL) and high-fat, high-cholesterol (HFHC) diet-fed mice (A), and in CTRL and methionine- and choline-deficient (MCD) diet-fed mice (B). Serum epoxyeicosatrienoic acids (EETs) were undetectable in both models. Dashed lines indicate the limits of detection. Values below the limit of detection were plotted at 0.001 ng/mL for visualization, precluding reliable statistical comparisons for 11,12-DHET and 8,9-DHET in panel A. n = 6 per group. Statistical significance was determined using unpaired Student's *t*-test. Reliable statistical comparisons for 11,12-DHET and 8,9-DHET in panel A.

Fig. S6

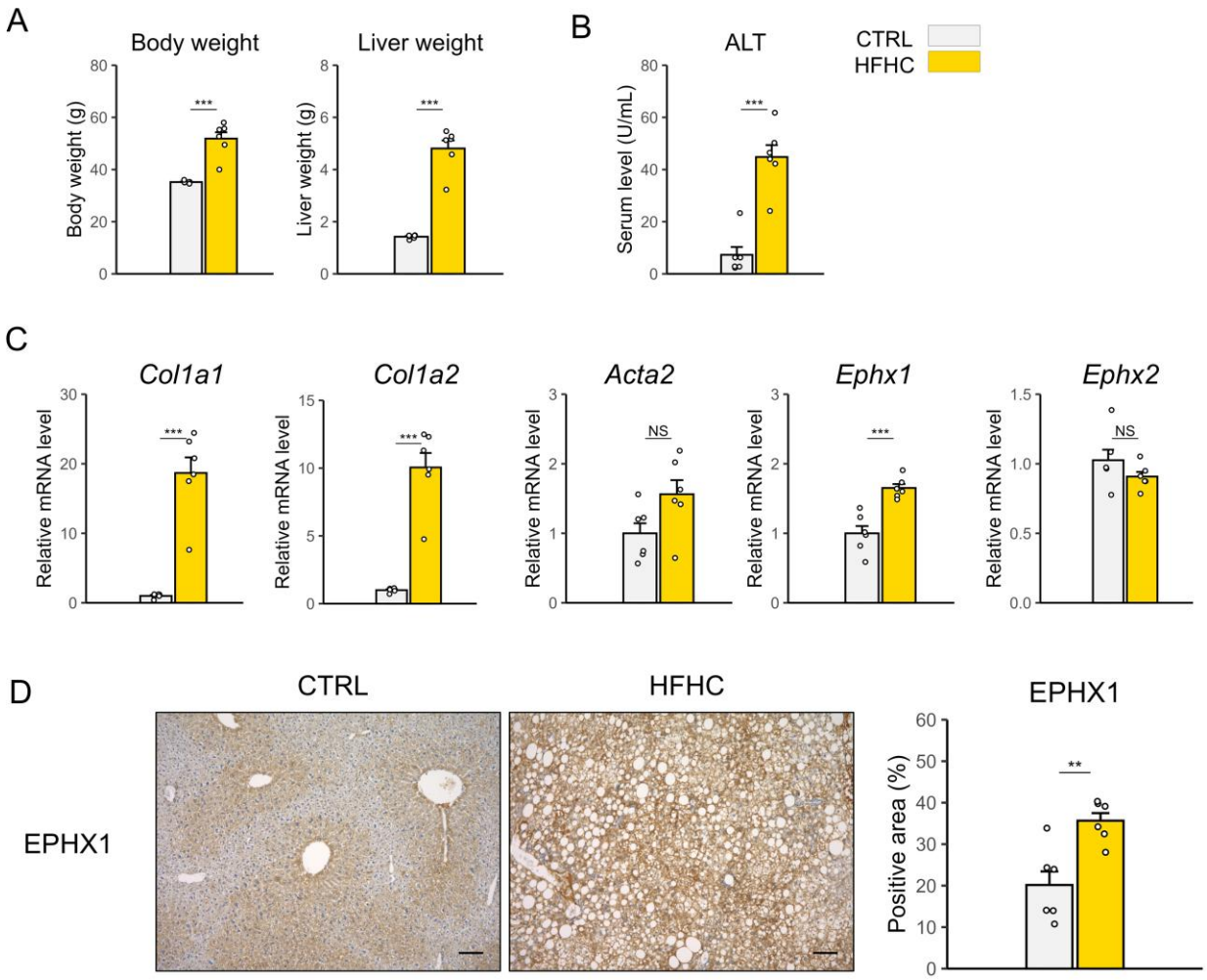


Fig. S6. Body weight, liver weight, *serum ALT levels, hepatic gene expression*, and immunohistochemical appearance against microsomal epoxide hydrolase (EPHX1) in high-fat, high-cholesterol (HFHC) diet-induced fibrotic mouse model.

(A) Changes in body weight and liver weight. (B) Serum alanine transaminase (ALT) levels. (C) mRNA levels of *Col1a1, Col1a2, Acta2, Ephx1* and *Ephx2*. (D) Representative images of EPHX1 immunohistochemical staining and quantification of the EPHX1-positive area. Scale bar, 100 μm. n = 6 per group. Statistical significance was determined using unpaired Student's *t*-test. * $p < 0.05$, ** $p < 0.01$, *** $p < 0.001$. NS, not significant.

Fig. S7

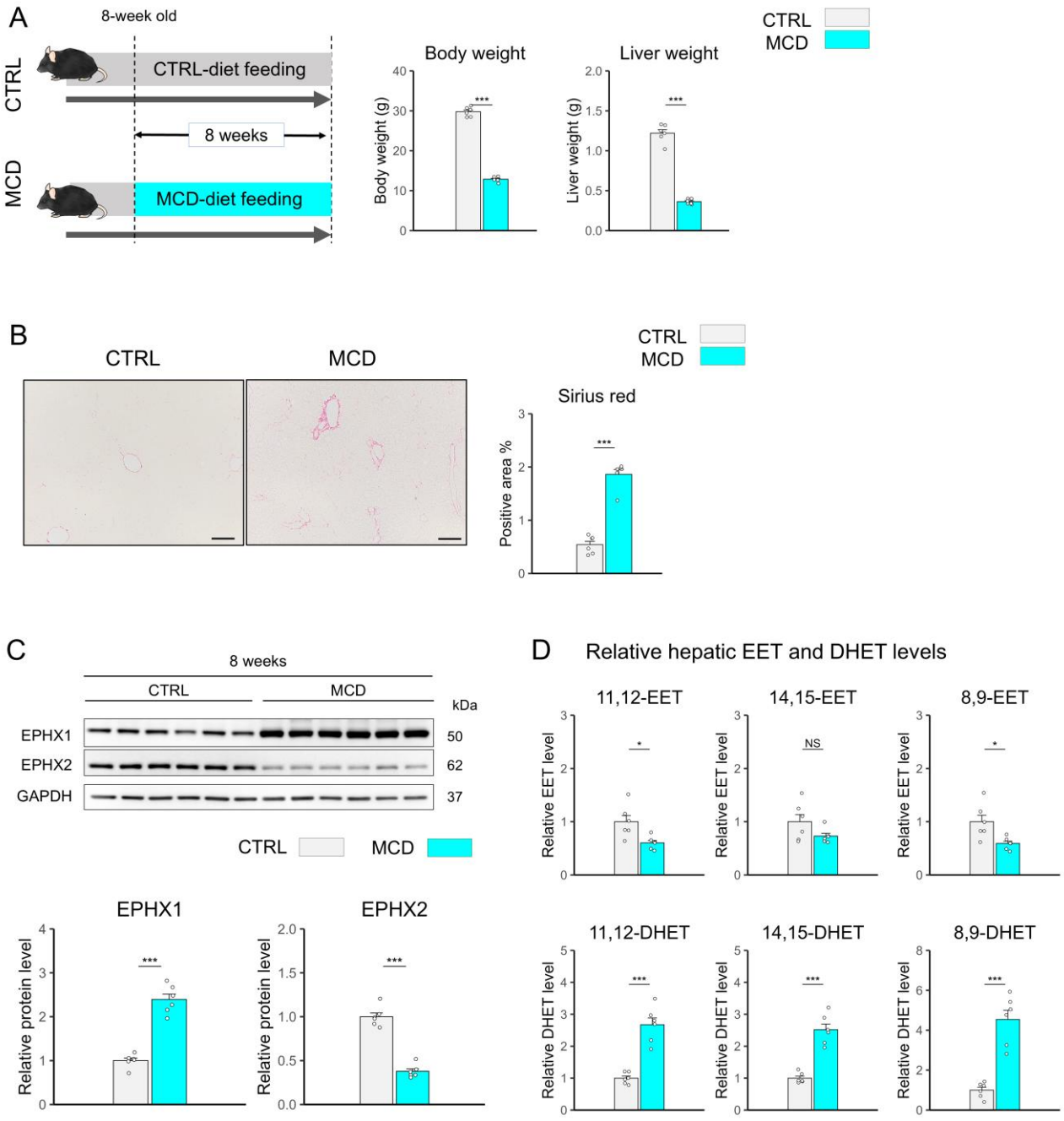


Fig. S7. Hepatic microsomal epoxide hydrolase (EPHX1), soluble epoxide hydrolase (EPHX2), dihydroxyeicosatrienoic acid (DHET), and epoxyeicosatrienoic acid (EET) in methionine and choline-deficient (MCD) fibrotic mouse model.

(A) Fibrotic mouse model by feeding an MCD diet for 8 weeks were generated. Changes in body weight and liver weight. (B) Sirius red staining of liver tissue (left) and digital morphometric

measurements of Sirius red-positive area (right). Scale bar, 100 μm. (C) Western blot analysis of EPHX1 and EPHX2 in the livers of MCD-fed mice compared with those of CTRL mice. The protein levels were quantified using ImageJ software. The values were normalized to the protein levels of glyceraldehyde-3-phosphate dehydrogenase (GAPDH). (D) Hepatic EET and DHET levels in MCD-fed mice compared with control (CTRL) mice. Columns and bars represent mean and standard error, respectively. n = 6. Statistical significance was determined using an unpaired Student's *t*-test or Pearson's correlation test. * $p < 0.05$, ** $p < 0.01$, *** $p < 0.001$. NS, not significant.

Fig. S8

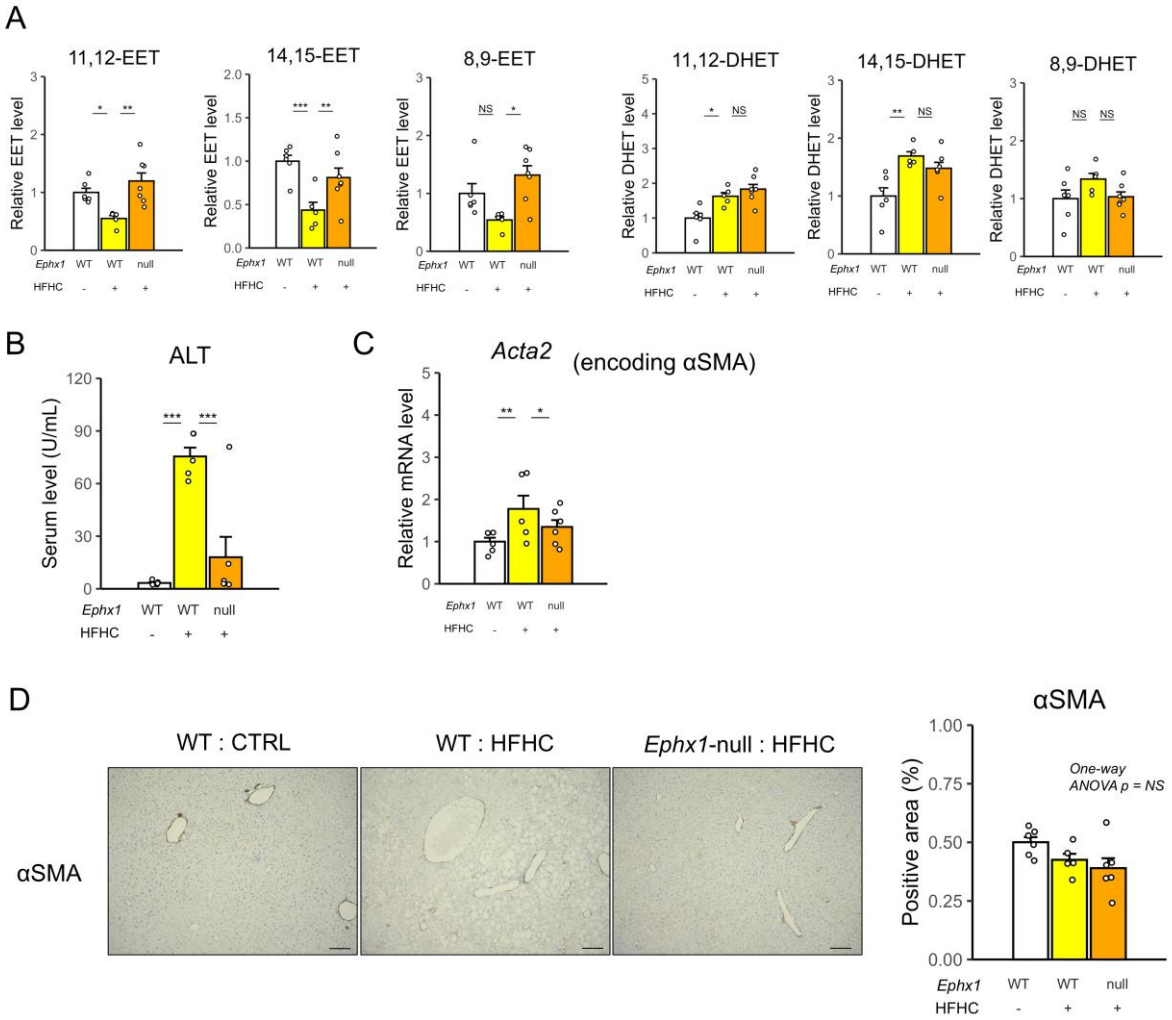


Fig. S8. Hepatic epoxyeicosatrienoic acid (EET) and dihydroxyeicosatrienoic acid (DHET) levels, serum ALT levels, and hepatic *Acta2* and alpha-smooth muscle actin (αSMA) expression in high-fat, high-cholesterol (HFHC)-fed *Ephx1*-null mice.

(A) Hepatic EET and DHET levels. (B) Serum alanine aminotransferase (ALT) levels. (C) Hepatic *Acta2* mRNA expression. (D) Representative images of αSMA immunohistochemical staining and quantification of the αSMA-positive area. CTRL, control. n = 5−6. Scale bar, 100 μm. Columns and bars represent mean and standard error, respectively. Statistical significance was calculated using one-way ANOVA with Tukey's post hoc test. * $p < 0.05$, ** $p < 0.01$, *** $p < 0.001$. NS, not significant.

Fig. S9

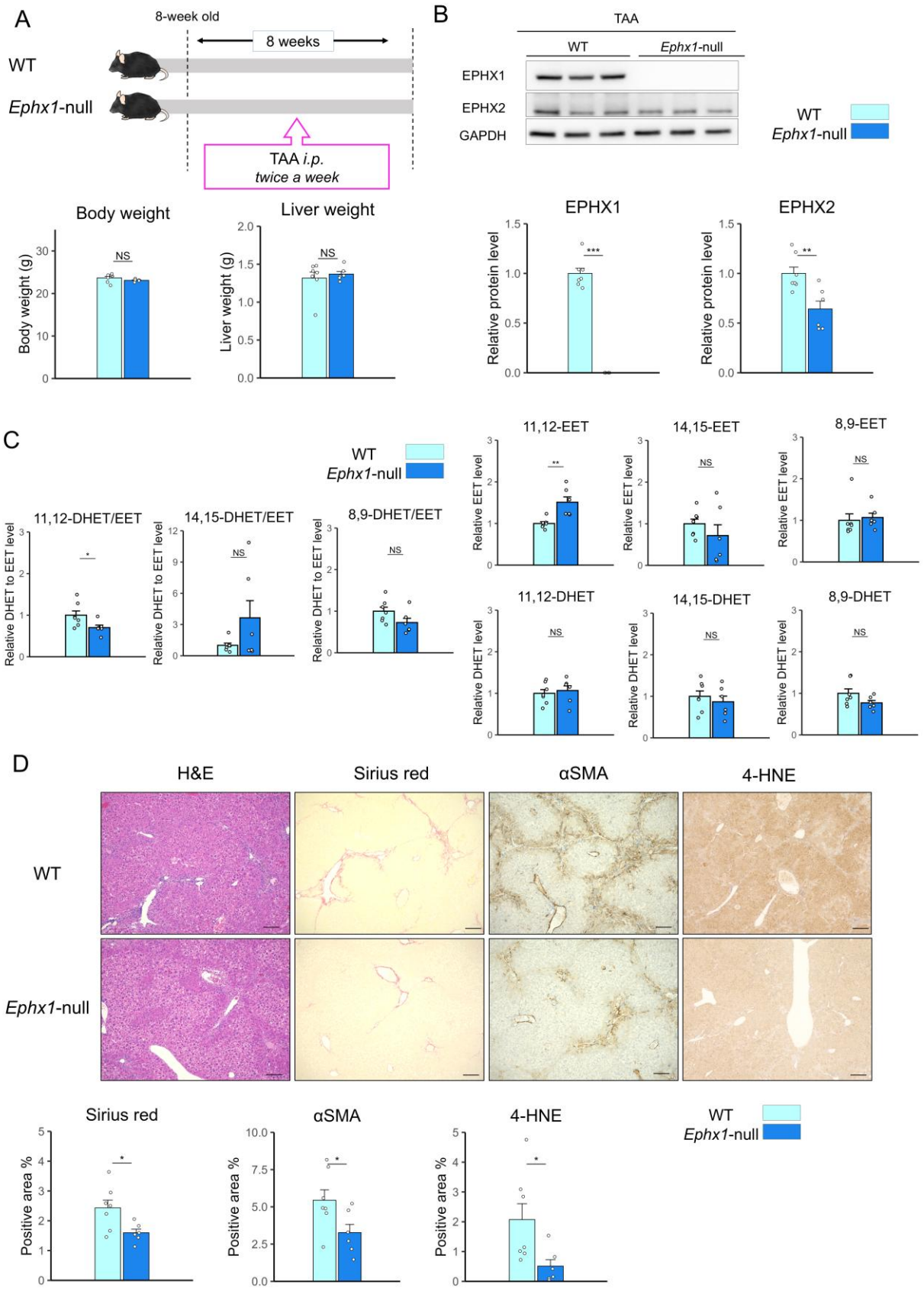

A
8-week old
8 weeks
WT
Ephx1-null
TAA i.p.
twice a week
B
TAA
WT
Ephx1-null
EPHX1
EPHX2
GAPDH
WT
Ephx1-null
Body weight
Body weight (g)
NS
Liver weight
Liver weight (g)
NS
EPHX1
Relative protein level
***
EPHX2
Relative protein level
**
C
WT
Ephx1-null
11,12-DHET/EET
Relative DHET to EET level
*
14,15-DHET/EET
Relative DHET to EET level
NS
8,9-DHET/EET
Relative DHET to EET level
NS
11,12-EET
Relative EET level
**
14,15-EET
Relative EET level
NS
8,9-EET
Relative EET level
NS
11,12-DHET
Relative DHET level
NS
14,15-DHET
Relative DHET level
NS
8,9-DHET
Relative DHET level
NS
D
H&E
Sirius red
αSMA
4-HNE
WT
Ephx1-null
Sirius red
Positive area %
*
αSMA
Positive area %
*
4-HNE
Positive area %
*
WT
Ephx1-null

Fig. S9. Hepatic epoxyeicosatrienoic acid (EET) metabolism and liver fibrogenesis in thioacetamide (TAA)-administered *Ephx1*-null mice.

(A) Experimental design and body and liver weights of wild-type (WT) and *EPHX1*-null mice after 8 weeks of intraperitoneal (*i.p.*) TAA administration. (B) Hepatic EPHX1 and EPHX2 levels. (C) Hepatic dihydroxyeicosatrienoic acid (DHET)/EET ratio as indices of EET hydrolysis and relative hepatic EET and DHET levels. (D) Sections stained with hematoxylin and eosin (H&E) or Sirius red, or immunostained for alpha-smooth muscle actin (αSMA) or 4-hydroxynonenal (4-HNE), and quantification of staining intensity. n = 6−7 per group. Scale bar, 100 μm. Columns and bars represent mean and standard error, respectively. Statistical significance was determined using an unpaired Student's *t*-test. * $p < 0.05$, ** $p < 0.01$, *** $p < 0.001$. NS, not significant.

Fig. S10

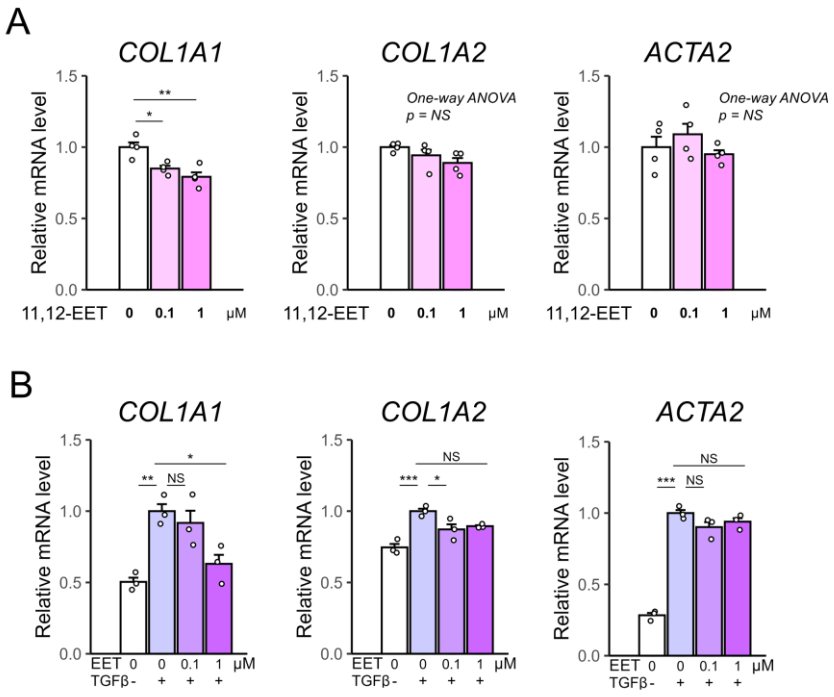


Fig. S10. Fibrotic gene expression in Effect of 11,12-epoxyeicosatrienoic acid (EET) on human hepatic stellate cells (HSCs). (A, B) *COL1A1*, *COL1A2*, and *ACTA2* mRNA levels in human HSC lines after treatment with 11,12-EET (A) and under TGF-β stimulation (B). Statistical significance was determined using one-way ANOVA with Dunnett's post-hoc test. Columns and bars represent mean and standard error, respectively. * $p < 0.05$, ** $p < 0.01$, *** $p < 0.001$. NS, not significant.

Fig. S11

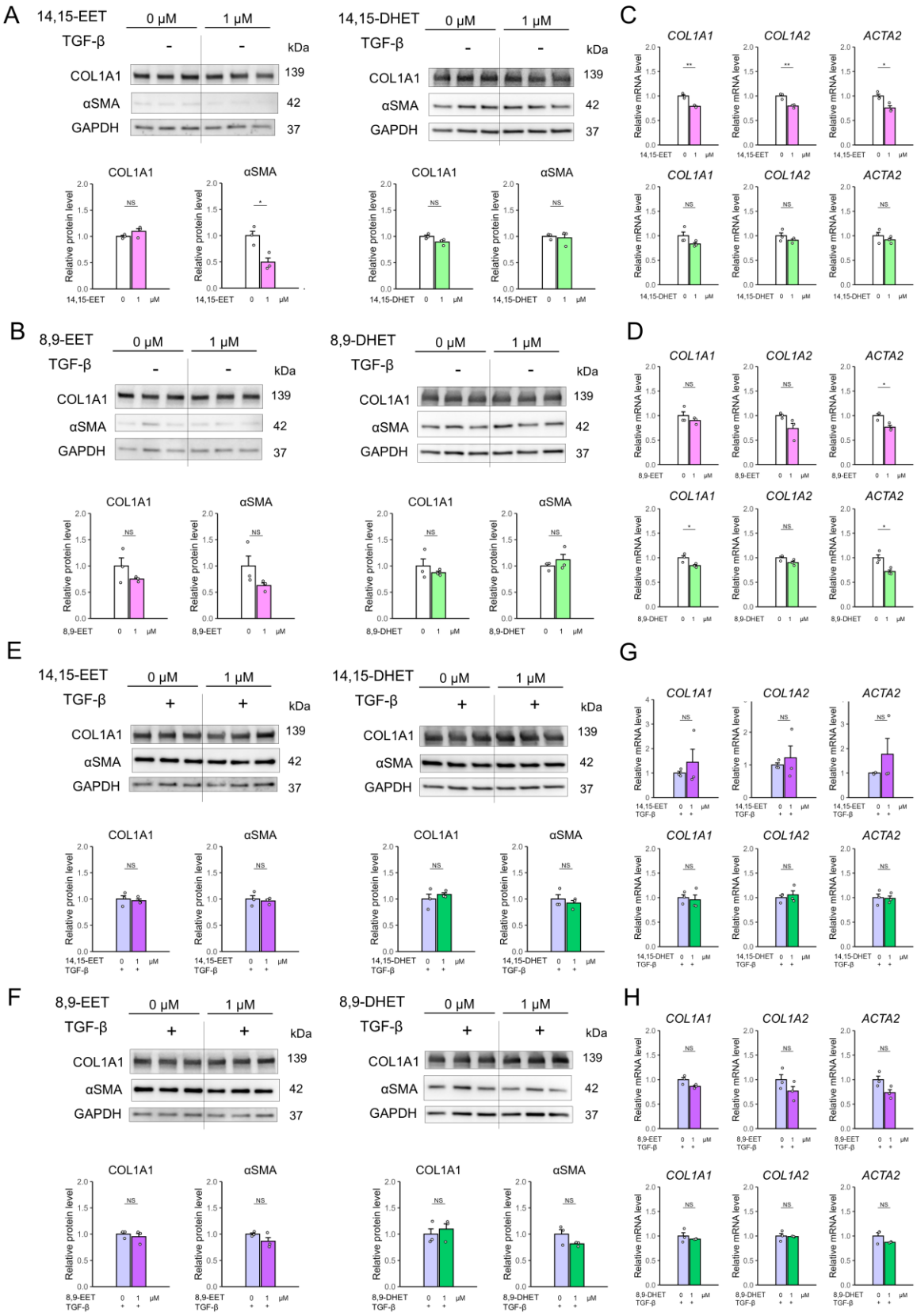

A
14,15-EET
0 μM
1 μM
TGF-β
kDa
COL1A1
αSMA
GAPDH
139
42
37
14,15-DHET
B
8,9-EET
8,9-DHET
C
D
E
F
G
H
COL1A2
ACTA2
Relative protein level
Relative mRNA level
NS

Fig. S11. Effects of 14,15-epoxyeicosatrienoic acid (EET), 14,15-dihydroxyeicosatrienoic acid (DHET), 8,9-EET, and 8,9-DHET on human hepatic stellate cells (HSCs). (A, B) COL1A1 and alpha-smooth muscle actin (αSMA) protein levels in HSCs treated with 14,15-EET or 14,15-DHET (A) and 8,9-EET or 8,9-DHET (B). (C, D) *COL1A1*, *COL1A2*, and *ACTA2* mRNA levels in HSCs treated with 14,15-EET or 14,15-DHET (C) and 8,9-EET or 8,9-DHET (D). (E, F) COL1A1 and αSMA protein levels in HSCs under transforming growth factor-β (TGF-β) stimulation with 14,15-EET or 14,15-DHET (E), and with 8,9-EET or 8,9-DHET (F). (G, H) *COL1A1*, *COL1A2*, and *ACTA2* mRNA levels in HSCs under TGF-β stimulation with 14,15-EET or 14,15-DHET (G) and with 8,9-EET or 8,9-DHET (H). Statistical significance was determined using an unpaired Student's *t*-test. Columns and bars represent mean and standard error, respectively. * $p < 0.05$, ** $p < 0.01$, *** $p < 0.001$. NS, not significant.

Fig. S12

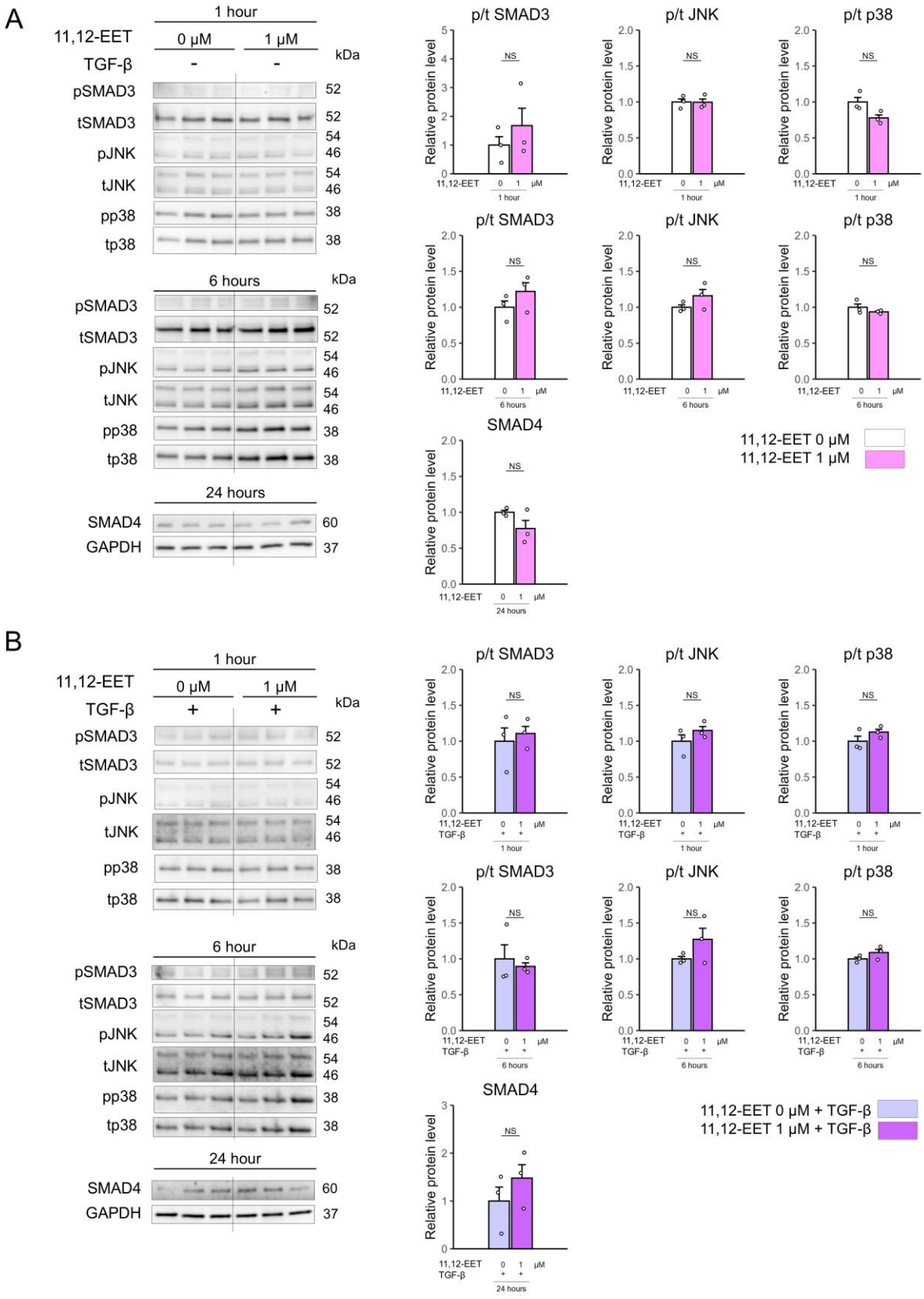

A
1 hour
11,12-EET
0 μM
1 μM
TGF-β
-
-
kDa
pSMAD3
tSMAD3
pJNK
tJNK
pp38
tp38
52
52
54
46
54
46
38
38
6 hours
24 hours
SMAD4
GAPDH
60
37
p/t SMAD3
p/t JNK
p/t p38
Relative protein level
NS
11,12-EET
0 1 μM
1 hour
6 hours
24 hours
11,12-EET 0 μM
11,12-EET 1 μM
B
1 hour
6 hour
24 hour
+
+
TGF-β
11,12-EET 0 μM + TGF-β
11,12-EET 1 μM + TGF-β

Fig. S12. Effects of 11,12-epoxyeicosatrienoic acid (EET) on signaling pathways in human hepatic stellate cells with or without transforming growth factor-β (TGF-β) stimulation.

(A) SMAD3, c-Jun N-terminal kinase (JNK), and p38 phosphorylation at 1 and 6 hours and SMAD4 expression at 24 hours after treatment with 11,12-EET. (B) The same analyses in HSCs under TGF-β stimulation. Statistical significance was determined using an unpaired Student's *t*-test. Columns and bars represent mean and standard error, respectively. * $p < 0.05$, ** $p < 0.01$, *** $p < 0.001$. NS, not significant.

Fig. S13

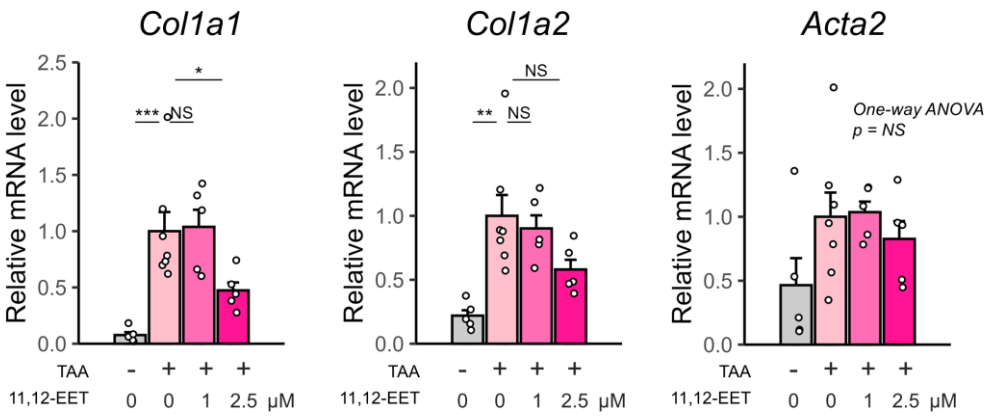


Fig. S13. Effects of 11,12-epoxyeicosatrienoic acid (EET) on hepatic fibrogenic gene expression in thioacetamide (TAA)-induced liver fibrosis.

Hepatic *Col1a1*, *Col1a2*, and *Acta2* mRNA levels in control mice and TAA-treated mice receiving vehicle or 11,12-EET at 1 or 2.5 μM. One-way ANOVA with Dunnett's post hoc test. Columns and bars represent mean and standard error, respectively. * $p < 0.05$, ** $p < 0.01$, *** $p < 0.001$. NS, not significant.

Fig. S14

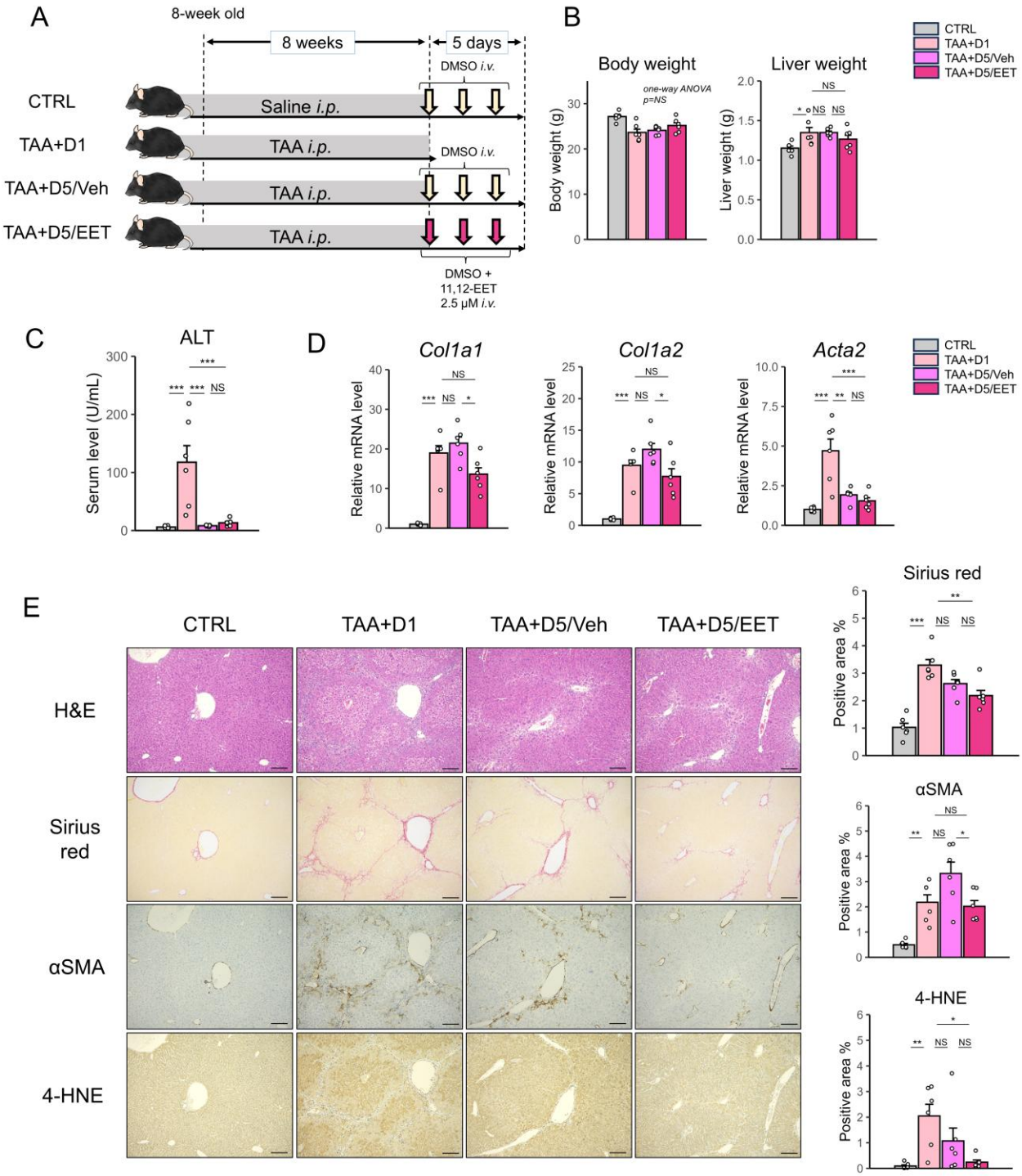


Fig. S14. Effects of 11,12-epoxyeicosatrienoic acid (EET) treatment after establishment of thioacetamide (TAA)-induced liver fibrosis.

(A) Experimental design. Mice were divided into four groups: CTRL, mice receiving intraperitoneal saline injections only; TAA+D1, mice sacrificed 1 day after the final TAA injection as the baseline group; TAA+D5/Veh, mice administered saline containing 0.5% dimethyl sulfoxide (DMSO) on days 0, 2, and 4 after the final TAA injection and sacrificed on day 5; and TAA+D5/EET, mice administered 2.5 μM 11,12-EET in saline containing 0.5% DMSO on days 0, 2, and 4 and sacrificed on day 5. (B) Body and liver weights. (C) Serum alanine aminotransferase (ALT) levels. (D) Hepatic *Col1a1*, *Col1a2*, and *Acta2* mRNA expression. (E) Liver sections stained with hematoxylin and eosin (H&E) or Sirius red, or immunostained for α-smooth muscle actin (αSMA) or 4-hydroxynonenal (4-HNE). Scale bar, 100 μm. Statistical significance was calculated using an one-way ANOVA with Tukey's post hoc test. Columns and bars represent mean and standard error, respectively. * $p < 0.05$, ** $p < 0.01$, *** $p < 0.001$. NS, not significant.

Fig. S15

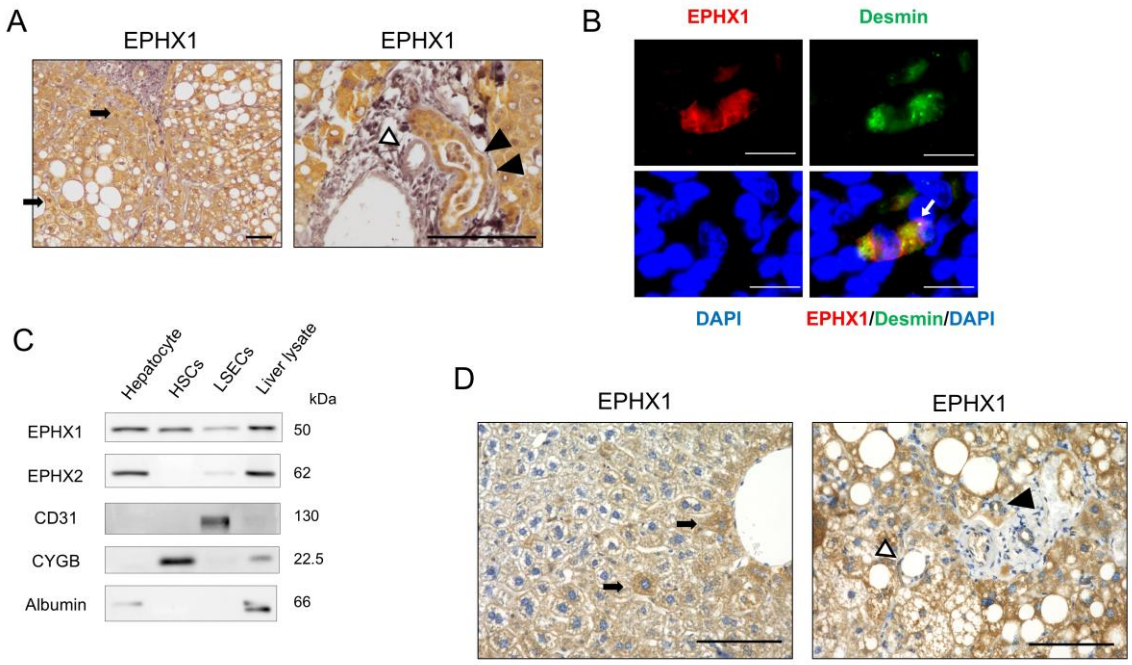


Fig. S15. Cellular distribution of microsomal epoxide hydrolase 1 (EPHX1) in human and mouse liver.

(A) Representative images of EPHX1 immunohistochemical staining in human liver. Scale bar, 100 μm. (B) Immunofluorescence staining of EPHX1 and desmin. Arrow, $EPHX1^{+}desmin^{+}$ cells. Nuclei were stained with DAPI. Scale bar, 5 μm. (C) EPHX1 and soluble epoxide hydrolase (EPHX2) expression in mouse primary hepatocytes, hepatic stellate cells (HSCs) and liver sinusoidal endothelial cells (LSEC). CD31, cytoglobin (CYGB), and albumin were used as markers for LSECs, HSCs, and hepatocytes, respectively. (D) Representative images of EPHX1 immunohistochemical staining in mouse liver. Scale bar, 100 μm. Arrows indicate hepatocytes, filled arrowheads indicate bile duct epithelial cells, and open arrowheads indicate vascular endothelial cells.

Fig. S16

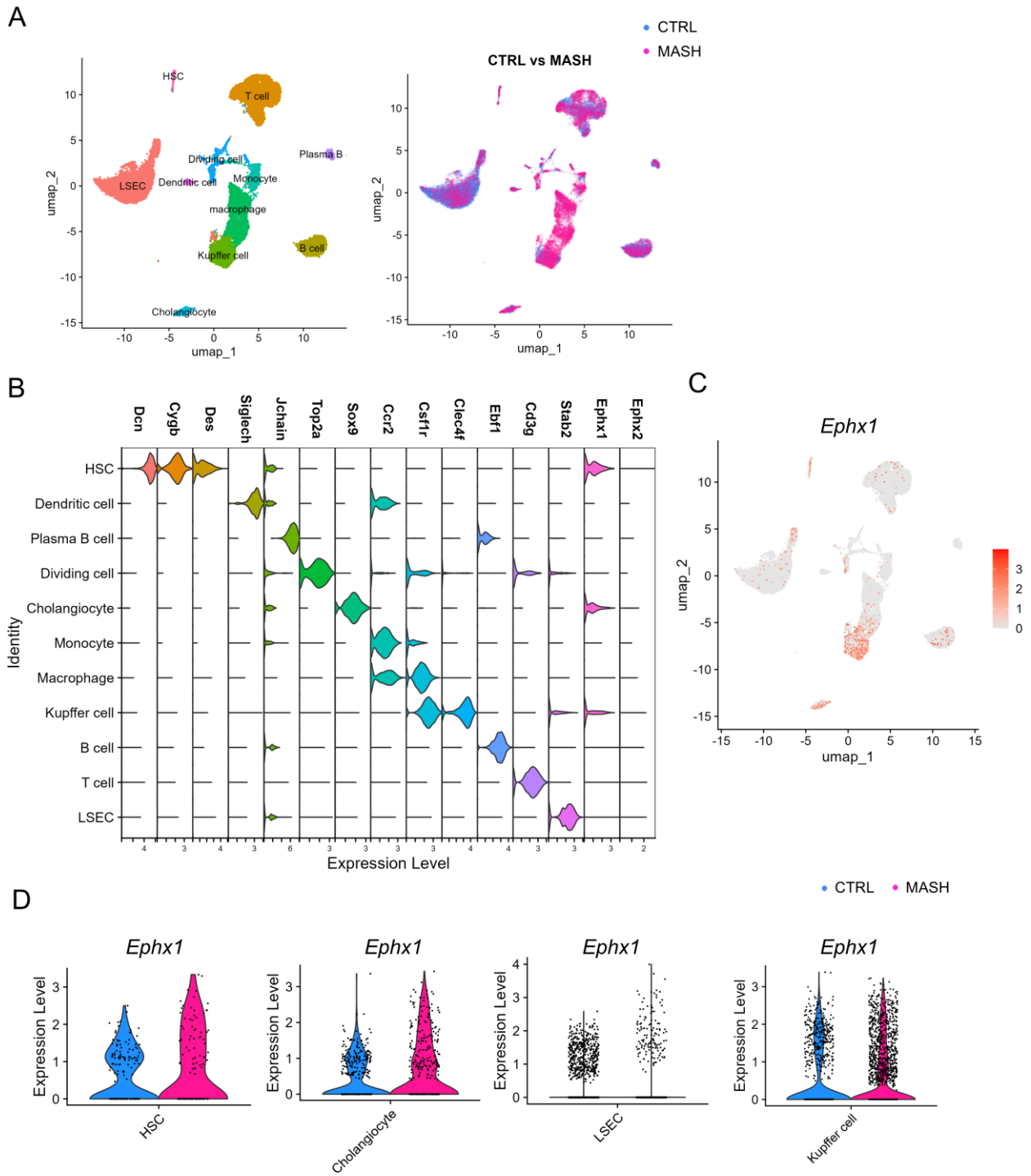


Fig. S16. Single-cell RNA-sequencing analysis of *Ephx1* expression in nonparenchymal liver cells from control and metabolic dysfunction-associated steatohepatitis (MASH) model mice.

Single-cell RNA-sequencing of the non-parenchymal cells from control (CTRL) and MASH model mice. The UMAP plots show annotations for cell types and group origin (A). Violin plots showing *Ephx1*, *Ephx2*, and marker genes for 14 distinct cell types (B). Feature plots of *Ephx1* (C). Violin plots of *Ephx1* in hepatic stellate cell (HSC), cholangiocyte, liver sinusoidal endothelial cell (LSEC) and Kupffer cell clusters (D). *Ephx1*, microsomal epoxide hydrolase 1; *Ephx2*, soluble epoxide hydrolase 2.

Fig. S17

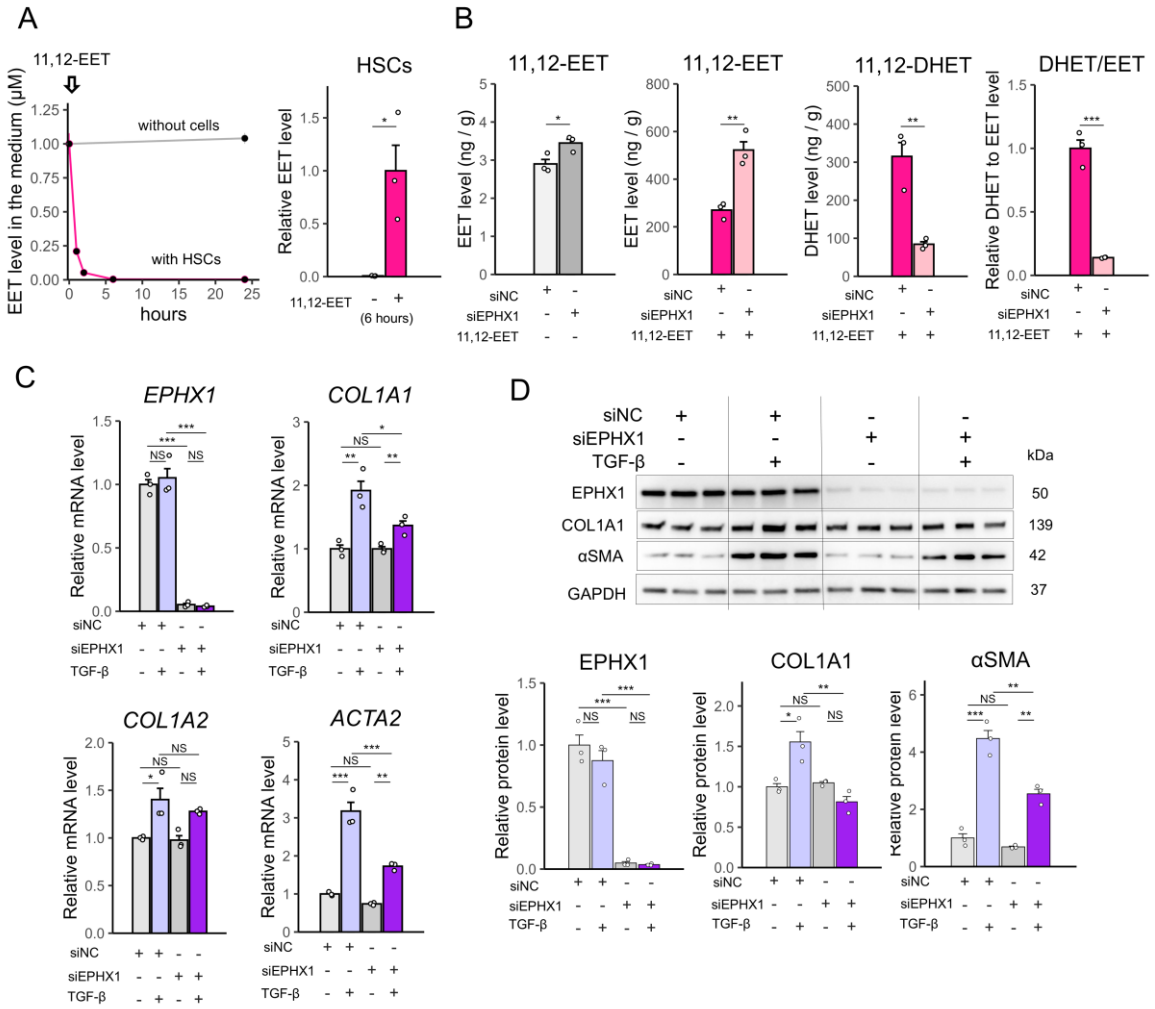


Fig. S17. Effect of EPHX1 knockdown on 11,12-epoxyeicosatrienoic acid (EET) metabolism and fibrogenic response in human hepatic stellate cells (HSCs).

(A) 11,12-EET levels in the medium after the addition of 11,12-EET to HSCs, and that in the HSCs. (B) Metabolites levels in HSCs treated with siEPHX1 and 11,12-EET. Effect of siEPHX1 on *EPHX1* and collagen mRNA expression (C), and protein expression with TGF-β stimulation (D). Statistical significance was determined by an unpaired Student's t test or one-way ANOVA with Turkey's post hoc test. Each column and bar represent the mean and standard error, respectively. * $p < 0.05$, ** $p < 0.01$, *** $p < 0.001$. NS, not significant.

Supplementary Tables

Table S1. Baseline patient characteristics for lipidome analysis in patients with MASLD.

Variables	Mild fibrosis n = 55	Advanced fibrosis n = 47	*p* value
Age (years)	60 [52, 69]	63 [56, 68]	0.31
Sex: Male	27 (49.1)	17 (36.2)	0.19
BMI (kg/m^2)	26.9 [25.0, 28.7]	29.0 [26.2, 30.9]	0.05*
Diabetes	20 (36.4)	23 (48.9)	0.20
Hyperlipidemia	30 (54.5)	25 (53.2)	0.89
FIB-4 index	1.98 [1.12, 2.70]	3.18 [2.22, 4.31]	<0.001***
Platelet count ($10^3/\mu L$)	200 [165, 238]	164 [133, 205]	0.008**
INR	0.95 [0.92, 1.00]	1.03 [1.00, 1.08]	<0.001***
Albumin (g/dL)	4.1 [4.0, 4.3]	4.0 [3.8, 4.3]	0.19
Bilirubin (mg/dL)	0.7 [0.6, 1.0]	0.8 [0.7, 1.1]	0.08
ALT (U/L)	89 [55, 128]	69 [50, 109]	0.14
Hemoglobin (g/dL)	14.5 [13.7, 15.6]	14.0 [13.1, 14.9]	0.09
Creatinine (mg/dL)	0.71 [0.64, 0.88]	0.69 [0.57, 0.80]	0.16
MAS 2 / 3 / 4 / 5 / 6 / 7 / 8	0 / 4 / 18 / 20 / 9 / 3 / 1	2 / 0 / 11 / 14 / 15 / 3 / 2	0.12

Values are reported as n (%) or median [interquartile range].

Abbreviations: ALT, alanine aminotransferase; BMI, body mass index; FIB-4 index, fibrosis-4 index; INR, prothrombin time-international normalized ratio; MAS, MASLD activity score; MASLD, metabolic dysfunction–associated steatotic liver disease. * $p < 0.05$, ** $p < 0.01$, *** $p < 0.001$.

Table S2. Baseline patient characteristics for lipidome analysis in patients with chronic hepatitis C.

Variables	Mild fibrosis n = 40	Advanced fibrosis n = 81	*p* value
Age (years)	67 [62, 75]	69 [63, 76]	0.40
Sex: Male	15 (37.5)	41 (50.6)	0.17
BMI (kg/m^2)	22.7 [20.8, 24.8]	23.1 [21.6, 25.7]	0.36
Diabetes	7 (17.5)	18 (22.5)	0.53
Hyperlipidemia	6 (15.0)	6 (7.7)	0.21
LSM by VCTA (kPa)	7.1 [5.4, 8.9]	19.4 [14.0, 25.1]	<0.001***
FIB-4 index	2.66 [2.18, 3.39]	5.83 [3.90, 8.14]	<0.001***
Platelet count ($10^3/\mu L$)	171 [130, 209]	100 [76, 154]	<0.001***
INR	1.01 [0.97, 1.06]	1.06 [1.02, 1.11]	<0.001***
Albumin (g/dL)	4.1 [3.9, 4.4]	3.8 [3.4, 4.0]	<0.001***
Bilirubin (mg/dL)	0.6 [0.5, 0.8]	0.8 [0.6, 1.1]	0.003**
ALT (U/L)	41 [27, 65]	46 [36, 76]	0.14
Hemoglobin (g/dL)	13.8 [13.0, 14.4]	13.5 [12.0, 14.3]	0.21
Creatinine (mg/dL)	0.68 [0.55, 0.82]	0.72 [0.62, 0.84]	0.11
Genotype 1 / 2	30 / 10	62 / 19	0.85
HCV-RNA (logIU/mL)	6.2 [5.7, 6.7]	6.2 [5.9, 6.4]	0.62

Values are reported as n (%) or median [interquartile range].

Abbreviations: ALT, alanine aminotransferase; BMI, body mass index; FIB-4 index, fibrosis-4 index; HCV, hepatitis C virus; INR, prothrombin time-international normalized ratio; LSM, liver stiffness measurement; VCTA, vibration-controlled transient elastography. * $p < 0.05$, ** $p < 0.01$, *** $p < 0.001$.

Table S3. Univariate and multivariate logistic regression analyses of factors used to differentiate between chronic hepatitis C patients with or without advanced fibrosis.

Variables		Univariate			Multivariate		
		OR	95% CI	*p* value	OR	95% CI	*p* value
11,12-DHET	per 0.1 ng/mL	1.48	1.13–1.94	0.004**	1.39	1.02–1.89	0.03*
14,15-DHET	per 0.1 ng/mL	2.03	1.35–3.06	<0.001***			
8,9-DHET	per 0.1 ng/mL	1.86	1.17–2.93	0.008**			
Age	per 10 years	1.19	0.80–1.77	0.39			
Sex	Male	1.71	0.79–3.71	0.18			
BMI	per 1 kg/m^2	1.06	0.96–1.17	0.24	1.15	0.99–1.35	0.07
FIB-4 index	per 1	2.16	1.57–2.98	<0.001***	1.80	1.22–2.67	0.003**
Albumin	per 1 g/dL	0.77	0.68–0.86	<0.001***	0.14	0.03–0.69	0.02*
Bilirubin	per 1 mg/dL	7.49	1.82–30.91	0.005**	7.57	0.91–63.3	0.06
ALT	per 10 U/L	1.00	0.93–1.07	0.94	0.98	0.89–1.08	0.70

Abbreviations: ALT, alanine aminotransferase; BMI, body mass index; CI, confidence interval; DHET, dihydroxyeicosatrienoic acid; FIB-4 index, fibrosis-4 index; OR, odds ratio. * $p < 0.05$, ** $p < 0.01$, *** $p < 0.001$.

Table S4. Baseline patient characteristics for immunohistochemistry staining in patients with MASLD.

Variables	No advanced fibrosis n = 24	Advanced fibrosis n = 24	*p* value
Age (years)	61 [56, 65]	65 [58, 68]	0.32
Sex: Male	11 (45.8)	9 (37.5)	0.56
BMI (kg/m^2)	27.7 [25.9, 28.7]	28.2 [24.4, 31.2]	0.59
Diabetes	8 (33.3)	14 (58.3)	0.08
Hyperlipidemia	11 (45.8)	12 (50.0)	0.77
FIB-4 index	1.93 [1.14, 2.59]	3.07 [2.59, 4.39]	<0.001***
Platelet count ($10^3/\mu L$)	219 [181, 243]	155 [118, 202]	0.005**
INR	0.97 [0.93, 1.02]	1.05 [1.01, 1.11]	<0.001***
Albumin (g/dL)	4.2 [4.1, 4.4]	4.1 [3.9, 4.3]	0.15
Bilirubin (mg/dL)	0.7 [0.6, 1.0]	0.8 [0.7, 1.2]	0.14
ALT (U/L)	84 [44, 133]	72 [42, 109]	0.23
Hemoglobin (g/dL)	14.9 [13.8, 15.5]	14.4 [13.1, 15.2]	0.23
Creatinine (mg/dL)	0.72 [0.62, 0.90]	0.70 [0.59, 0.75]	0.50
Fibrosis stage 1 / 2 / 3 / 4	11 / 13 / 0 / 0	0 / 0 / 12 / 12	<0.001***
MAS 2 / 3 / 4 / 5 / 6 / 7 / 8	1 / 4 / 12 / 5 / 2 / 0	1 / 1 / 4 / 9 / 6 / 3	0.04*

Values are reported as n (%) or median [interquartile range].
We defined advanced fibrosis as histological fibrosis stage 3–4. Histological fibrosis stage and MAS were defined by the NASH Clinical Research Network scoring system in patients with MASLD.
Abbreviations: ALT, alanine aminotransferase; BMI, body mass index; FIB-4 index, fibrosis-4 index; INR, prothrombin time-international normalized ratio; MAS, MASLD activity score; MASLD, metabolic dysfunction–associated steatotic liver disease. * $p < 0.05$, ** $p < 0.01$, *** $p < 0.001$.

Table S5. Baseline patient characteristics for immunohistochemistry staining in patients with chronic hepatitis C.

Variables	No advanced fibrosis n = 23	Advanced fibrosis n = 19	*p* value
Age (years)	61 [55, 67]	59 [55, 65]	0.92
Sex: Male	12 (52.2)	9 (47.4)	0.76
BMI (kg/m^2)	23.1 [21.1, 25.2]	22.8 [21.3, 25.2]	0.79
Diabetes	3 (13.0)	3 (15.8)	0.80
Hyperlipidemia	3 (13.0)	2 (10.5)	0.80
FIB-4 index	2.31 [1.51, 3.83]	3.70 [3.02, 4.34]	0.02*
Platelet count ($10^3/\mu L$)	178 [150, 244]	132 [112, 164]	0.007**
INR	0.99 [0.94, 1.04]	1.02 [0.99, 1.16]	0.06
Albumin (g/dL)	4.1 [4.0, 4.4]	3.9 [3.8, 4.3]	0.07
Bilirubin (mg/dL)	0.6 [0.4, 0.8]	0.8 [0.7, 1.0]	0.01*
ALT (U/L)	40 [27, 66]	68 [53, 122]	0.01*
Hemoglobin (g/dL)	13.8 [13.1, 14.5]	13.3 [12.4, 14.8]	0.43
Creatinine (mg/dL)	0.71 [0.56, 0.82]	0.70 [0.57, 0.80]	0.87
Histological grade of inflammation 0 / 1 / 2 / 3	3 / 11 / 9 / 0	1 / 6 / 8 / 4	0.10
Fibrosis stage 1 / 2 / 3 / 4	11 / 12 / 0 / 0	0 / 0 / 13 / 6	<0.001***

Values are reported as n (%) or median [interquartile range].

We defined advanced fibrosis as histological fibrosis stage 3–4. Histological fibrosis stage and grade of inflammation were defined by the METAVIR score.

Abbreviations: ALT, alanine aminotransferase; BMI, body mass index; FIB-4 index, fibrosis-4 index; INR, prothrombin time-international normalized ratio.

* $p < 0.05$, ** $p < 0.01$, *** $p < 0.001$.

Table S6. Univariate and multivariate logistic regression analyses of factors used to differentiate between chronic hepatitis C patients with or without advanced fibrosis.

		Univariate			Multivariate		
Variables		OR	95% CI	*p* value	OR	95% CI	*p* value
EPHX1	per 10% positive area	3.72	1.61–8.58	0.002**	4.02	1.49–10.9	0.006**
EPHX2	per 10% positive area	0.83	0.60–1.15	0.26			
CYP2C	per 10% positive area	1.17	0.72–1.90	0.54			
Age	per 10 years	1.08	0.52–2.21	0.84			
Sex	Male	0.83	0.24–2.79	0.76			
BMI	per 1 kg/m^2	0.95	0.80–1.13	0.57			
Platelet count	per $10^4/\mu L$	0.96	0.89–1.04	0.36			
FIB-4 index	per 1	1.68	1.07–2.64	0.02*	2.07	1.08–3.98	0.03*
Albumin	per 100 mg/dL	0.23	0.03–1.62	0.14			
Bilirubin	per 0.1 mg/dL	1.16	0.95–1.41	0.15			
ALT	per 10 U/L	1.11	0.99–1.25	0.07			
Histological grade of inflammation	per 1	2.53	1.04–6.16	0.04*	1.82	0.47–7.05	0.39

We defined advanced fibrosis as histological fibrosis stage 3–4. Histological fibrosis stage and grade of inflammation were defined by the METAVIR score.

Variables in multivariate analysis included EPHX1, FIB-4 index and histological grade of inflammation.

Abbreviations: ALT, alanine aminotransferase; BMI, body mass index; CI, confidence interval; CYP, cytochrome P450; EPHX1, microsomal epoxide hydrolase 1; EPHX2, soluble epoxide hydrolase 2; FIB-4 index, fibrosis-4 index; OR, odds ratio.

* $p < 0.05$, ** $p < 0.01$, *** $p < 0.001$

Table S7. Composition of CTRL and HFHC diets.

Component	CTRL diet (%)	HFHC diet (%)
Casein	14.0	25.60
L-cystine	0.18	0.36
Cornstarch	46.6	-
Alpha-cornstarch	15.5	16.00
Sucrose	10.0	5.50
Maltodextrin	-	6.00
Soybean oil	4.0	1.00
Lard	-	33.0
Cellulose powder	5.0	6.61
AIN-93G mineral	-	3.50
AIN-93M mineral	3.5	-
Calcium carbonate	-	0.18
AIN-93 vitamin	1.0	1.00
Choline bitartrate	0.25	0.25
Cholesterol	-	1.00
Tert-butylhydroquinone	0.0008	-

Abbreviations: CTRL, control; HFHC, high-fat high-cholesterol.

Table S8. Composition of CTRL and MCD diets.

Component	CTRL diet (%)	MCD diet (%)
L-isoleucine	0.921	0.921
L-leucine	1.59	1.59
L-lysine hydrochloride	1.70	1.70
L-methionine	0.510	-
L-cystine	0.082	0.082
L-phenylalanine	0.871	0.871
L-tyrosine	0.953	0.953
L-threonine	0.707	0.707
L-tryptophan	0.214	0.214
L-valine	1.15	1.15
L-histidine	0.51	0.51
L-arginine	0.625	0.625
L-alanine	0.510	0.510
L-aspartic acid	1.20	1.20
Glycine	0.312	0.312
L-proline	1.97	1.97
L-serine	0.888	0.888
L-aspartate	1.2	1.2
L-glutamate	3.62	3.622
Sucrose	40.0	40.0
Corn oil	10.0	10.0
Cellulose powder	5.0	5.0
AIN-93 vitamin	1.0	-
AIN-93 vitamin (without choline)	-	1.0
AIN-76 mineral	3.5	3.5
Tert-butylhydroquinone	0.002	0.002
Cornstarch	8.99	9.50
Alpha-cornstarch	13.2	13.2

Abbreviations: CTRL, control; MCD, methionine- and choline-deficient.

Table S9. Chemicals used in this study.

Name	Supplier	Catalogue number
14,15-EET (14,15-EpETrE)	Cayman Chemical	50651
11,12-EET (11,12-EpETrE)	Cayman Chemical	50511
8,9-EET (8,9-EpETrE)	Cayman Chemical	50351
14,15-DHT (14,15-DiHETrE)	Cayman Chemical	51651
11,12-DHT (11,12-DiHETrE)	Cayman Chemical	51511
8,9-DHT (8,9-DiHETrE)	Cayman Chemical	51351
5,8,11,14-Icosatetraenoic acid, peroxide free (arachidonic acid)	Cayman Chemical	90010.1
Prostaglandin E2-d4	Cayman Chemical	314010
Leukotriene B4-d4	Cayman Chemical	320110
Arachidonic acid-d8	Cayman Chemical	390010
Thioacetamide	Sigma-Aldrich	163678
siEPHX1	Dharmacon	M-008393-01-0010
siNC, GENOME Non-targeting siRNA Pools	Dharmacon	D-001206-13
RNAiMAX	ThermoFisher Scientific	13778-150
ROS Assay Kit -Highly Sensitive DCFH-DA-	Dojindo	340-09811

Abbreviations: EET, epoxyeicosatrienoic acid; DHT, dihydroxyeicosatrienoic acid; DiHOME, dihydroxyoctadecenoic acid.

Table S10. Antibodies used in this study.

Antibody	Supplier	Catalogue number	Species	Dilution
Immunohistochemical staining				
Anti-EPHX1 (mEH)	Santa Cruz Biotechnology	sc-135984	Mouse monoclonal	1/100
Anti-EPHX2 (sEH)	Santa Cruz Biotechnology	sc-166961	Mouse monoclonal	1/100
Anti-CYP2C8/9/18/19	Proteintech	16546-1-AP	Rabbit polyclonal	1/600
Anti-αSMA	Dako	M0851	Mouse monoclonal	1/200
Anti-4-HNE	Abcam	Ab46545	Rabbit polyclonal	1/50
Western blot analysis				
Anti-EPHX1 (mEH)	Santa Cruz Biotechnology	sc-135984	Mouse monoclonal	1/500
Anti-EPHX2 (she)	Santa Cruz Biotechnology	sc-166961	Mouse monoclonal	1/500
Anti-collagenI	Abcam	ab34710	Rabbit polyclonal	1/1000
Anti-GAPDH	Sigma-Aldrich	MAB374	Mouse monoclonal	1/10000
Anti-pSMAD3	Cell signaling	#9520	Rabbit monoclonal	1/1000
Anti-tSMAD3	Cell signaling	#9513	Rabbit polyclonal	1/1000
Anti-pJNK	Cell signaling	#4668	Rabbit monoclonal	1/1000
Anti-tJNK	Cell signaling	# 9258	Rabbit monoclonal	1/1000
Anti-pp38	Cell signaling	#9511	Rabbit polyclonal	1/1000
Anti-tp38	Cell signaling	#8690	Rabbit monoclonal	1/1000
Anti-CD31	R&D Systems	AF3628	Goat polyclonal	1/1000
Anti-albumin	Abcam	ab207327	Rabbit monoclonal	1/1000
Anti-CYGB	Our laboratory	Our laboratory[†]	Rabbit polyclonal	1/1000
Anti-αSMA	Dako	M0851	Mouse monoclonal	1/1000

Abbreviations: EPHX1 (mEH), microsomal epoxide hydrolase; EPHX2 (she), soluble epoxide hydrolase; CYP, cytochrome P450; GAPDH, glyceraldehyde-3-phosphate dehydrogenase; αSMA, α-smooth muscle actin; 4-HNE, 4-hydroxynonenal antibody; CYGB, cytoglobin; JNK, c-Jun N-terminal kinase.

[†]The anti-CYGB antibody was generated as described by Kawada et al. (J Biol Chem. 2001;276(27):25318–25323). CYGB was referred to as stellate cell activation-associated protein (STAP) in that report.

Table S11. Primers used in this study.

Gene	Forward (5′–3′)	Reverse (5′–3′)
Mouse *18S*	CGGCTACCACATCCAAGGAA	ATTGGAGCTGGAATTACCGC
Mouse *Ephx1*	GGAGACCTTACCACTTGAAGATG	GCCCGGAACCTATCTATCCTCT
Mouse *Ephx2*	GTCATCTACTGGTTTGTCTCCCG	GCCCGGAACCTATCTATCCTCT
Mouse *Col1a1*	GAGCGGAGAGTACTGGATCG	GTTCGGGCTGATGTACCAGT
Mouse *Col1a2*	TGTTGGCCCATCTGGTAAAGA	CAGGGAATCCGATGTTGCC
Mouse *Acta2*	TCCCTGGAGAAGAGCTACGAACT	AAGCGTTCGTTTCCAATGGT
Human *18S*	AGTCCCTGCCCTTTGTACACA	CGATCCGAGGGCCTCACTA
Human *EPHX1*	TGAGGAGATCCACGACTTACAC	CATTCCGCCAGTAGGAGATGA
Human *COL1A1*	AAGAGGAAGGCCAAGTCGAG	CACACGTCTCGGTCATGGTA
Human *COL1A2*	GAAAAGGAGTTGGACTTGGC	AGCAGGTCCTTGGAAACCTT
Human *ACTA2*	CCAGAGCCATTGTCACACAC	CAGCCAAGCACTGTCAGG